Analysis of residual stress in diamond films by x-ray diffraction and micro-Raman spectroscopy

N. G. Ferreira, E. Abramof, N. F. Leite, E. J. Corat, and V. J. Trava-Airoldi

Citation: J. Appl. Phys. **91**, 2466 (2002); doi: 10.1063/1.1431431
View online: http://dx.doi.org/10.1063/1.1431431
View Table of Contents: http://jap.aip.org/resource/1/JAPIAU/v91/i4
Published by the American Institute of Physics.

Analysis of residual stress in diamond films by x-ray diffraction and micro-Raman spectroscopy

N. G. Ferreira, E. Abramof, N. F. Leite, E. J. Corat, and V. J. Trava-Airoldi
Instituto Nacional de Pesquisas Espaciais, CP 515, 12201-970 São José dos Campos, SP, Brazil

(Received 6 July 2001; accepted for publication 6 November 2001)

We investigate the residual stress in diamond films grown on (001) silicon substrates as a function of film thickness. The diamond films were deposited at 1070 K by the conventional hot filament technique using a gas mixture of methane (1.0% vol) and hydrogen (99.0% vol). The film thickness, obtained from cross section scanning electron micrographs, varied from 3.0 to 42 μm as the growth time increased from 1 to 10 h. These images evidenced that the columnar growth is already established for films thicker than 10 μm. Top view micrographs revealed predominantly faceted pyramidal grains for the films at all growth stages. The grain size, obtained from these images, was found to vary linearly with film thickness. Using a high resolution x-ray diffractometer, the residual stress was determined by measuring, for each sample, the (331) diamond Bragg diffraction peak for Ψ values ranging from $-60°$ to $+60°$, and applying the $\sin^2\psi$ method. For the micro-Raman spectroscopy, we used the summation method, which consists in recording and adding a large number of spectra in different places of a selected area of the sample. All Raman spectra were fitted with Lorentzian lines to separate the contribution of the pure diamond and the other nondiamond (graphite) phases. This spectral analysis performed in each sample allowed the determination of the residual stress, from the diamond Raman peak shifts, and also the diamond purity, which increases from 70% to 90% as the thickness goes from 3 to 42 μm. The type and magnitude of the residual stress obtained from x-ray and micro-Raman measurements agreed well for films thicker than 10 μm. For films thinner than this value, an opposite behavior between both results was observed. We attributed this discrepancy to the domain size characteristic of each technique. © *2002 American Institute of Physics.* [DOI: 10.1063/1.1431431]

I. INTRODUCTION

Diamond films obtained by different chemical vapor deposition (CVD) techniques have demonstrated interesting and peculiar properties that make them appropriate for many technological applications. CVD diamonds are used, for instance, as a coating material in different tools,[1,2] as-doped electrodes,[3,4] or in optical windows.[5] The physical properties of the deposited films are strongly affected by the stress that usually remains after growth. Stressed films tend to split under tension and can even peel off from the substrate under compressive strain. It is then desirable to understand the origin and nature of the residual stresses in the CVD diamond films. Generally, the residual stress in these films is divided in two components. One is the thermal stress, which appears when the sample is cooled from growth down to room temperature, caused by the difference between the thermal expansion coefficients of film and substrate. Another is the intrinsic stress, which is built up during film growth, and is associated to the nondiamond material at the grain boundaries and to many structural defects, like impurities, micro twins, dislocations, etc.

The most common methods to determine the residual stress in diamond films are the substrate curvature technique,[6] x-ray diffraction[7,8] and Raman.[9] Particularly, Raman spectroscopy is a simple method that evaluates the residual stress through the diamond Raman peak shifts. However, when micro-Raman is used, it may present a difficult quantitative evaluation associated with the domain size effect[10] observed by the line shape and, also, multiple peaks may appear attributed to peak splitting due to a degeneracy of the optical phonons and the presence of inhomogeneous micro stresses. In order to obtain the residual stress by x-ray diffraction, the $\sin^2\psi$ technique is usually applied. This method allows determining the residual stress averaged over a larger sample area, and due to the transparency of diamond to x-ray, through the whole film depth.

Many authors have studied the stress in CVD diamond films grown by hot-filament[11–13] and microwave plasma.[6,14,15] The results generally show that the global intrinsic stress depends on the methane fraction, deposition temperature[6] and crystallographic orientation.[14] However, the understanding of residual stress formation in such films is incomplete and seems to be in a significant disagreement among various researchers as to the type and magnitude of the stress, even for similar deposition conditions. This divergence may be attributed to the stress measurement techniques, which generally have intrinsic limitations that should be considered.

In this paper, we investigate the residual stress in diamond films grown on (001) silicon substrates as function of film thickness. For this purpose, a series of CVD diamond films with thickness varying from 3 to 40 μm was grown by the hot-filament technique. A methane fraction of 1.0% was chosen and great care was taken to maintain the growth parameters constant and reproducible for all depositions. The

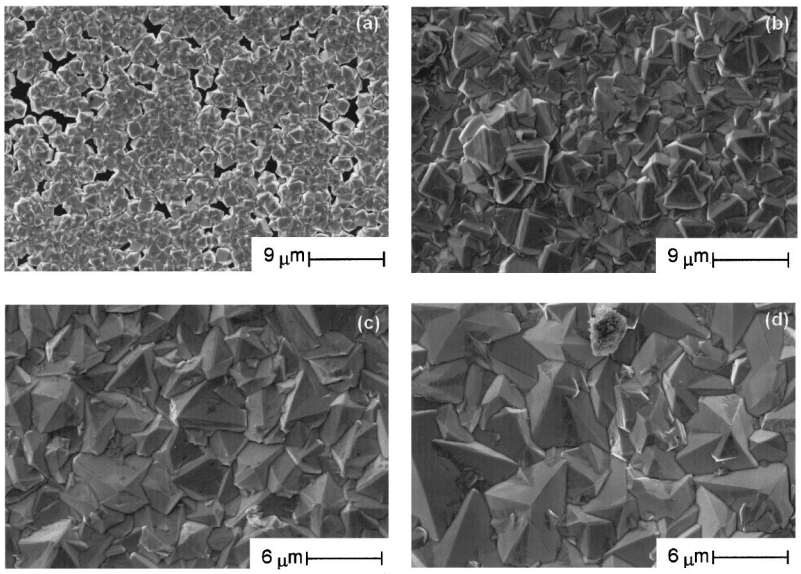

FIG. 1. Top view scanning electron micrographs, in the same magnification, for four diamond films grown during (a) 1, (b) 3, (c) 6.5 and (d) 10 h. The cross section images revealed film thickness of 3.0, 8.7, 21 and 42 μm, respectively. The surface morphology of all films exhibited predominantly faceted pyramidal grains.

only parameter that was varied was the growth time to obtain the different film thickness.

Scanning electron microscopy was performed to characterize structurally the grown films. Cross section micrographs were used to determine the film thickness and also to analyze the process of growth at the different stages. These images evidenced that, for films thicker than 10 μm, the columnar growth is completely established. Top view micrographs revealed predominantly faceted pyramidal grains for the films at all growth stages. The grain size, obtained from these images, was found to vary linearly with film thickness.

The total stress was determined by using two nondestructive techniques, namely, x-ray diffraction and micro-Raman spectroscopy. Using a high resolution x-ray diffractometer, $\Theta/2\Theta$ scans of the (331) diamond Bragg diffraction peak of all samples were measured for Ψ values ranging from $-60°$ to $+60°$, and the $\sin^2\psi$ method was applied. To get more reliable information from the micro-Raman spectroscopy, we used the summation method, which consists in recording and adding a large number of spectra in different places of a selected area of the sample. All Raman spectra were fitted with Lorentzian lines to separate the contribution of the pure diamond and the other nondiamond (graphite) phases. This spectral analysis performed in each sample allowed the determination of the residual stress; from the diamond Raman peak shifts, and also the diamond purity as a function of film thickness. We tried also to correlate the residual stress values with the diamond line broadening for the films with the different thickness.

The type and magnitude of the residual stress obtained from x-ray and micro-Raman measurements agreed well for films thicker than 10 μm. For films thinner than this value, an opposite behavior between both results was observed. We attributed this discrepancy to the domain size characteristic of each technique.

II. SAMPLE PREPARATION

Diamond films were deposited on silicon substrates by the conventional hot-filament technique using a gas mixture of methane (1.0% vol) and hydrogen (99.0% vol). The total flow rate was 100 sccm and the pressure inside the reactor was kept at 6.6×10^3 Pa. Substrates were cut from a single (001) type-*n* silicon wafer (1 Ω cm, 0.5 mm thick), which was pre-treated by a seeding process[16] using an ultrasonic bath of 0.25 μm diamond powder dispersed in hexane medium. The samples were grown at a temperature of 1070 K, measured by a thermocouple fixed at the bottom of the substrate, with growth duration times varying from 1 to 10 h. In order to keep all conditions unchanged from deposition to deposition, one filament was used for each deposition, and a special care was taken to maintain its form. The filament was placed at a distance of 5 mm to the substrate, and its temperature was 2470 K. The filaments were made of tungsten wire (diameter$=0.25$ m) with six coils 25 mm long. All of them were carbonized in a mixture of 1.0% CH_4 in H_2 with great care to avoid filament deformation. Deformed filaments were discarded. The films were characterized by scanning electron microscopy, x-ray diffraction and Raman spectroscopy. The experimental conditions and the main results are described below.

III. EXPERIMENTAL AND RESULTS

A. Scanning electron microscopy

The evaluation and interpretation of the stress data have strong dependence on the film characteristics. In order to investigate the morphology and texture, and to determine some important structural parameters, scanning electron microscopy (SEM) was performed using the microscopy System LEO 440. Top view and cross section micrographs were taken from all grown diamond films.

Figure 1 shows top view images, with the same magnification, of four CVD diamond films grown during 1.0, 3.0, 6.5 and 10 h. The surface morphology showed predominantly faceted pyramidal grains characteristic of the (111) textured growth. The grain size of each film was obtained by drawing the grains as small circles on the top view images. The average grain size was considered to be the mean value

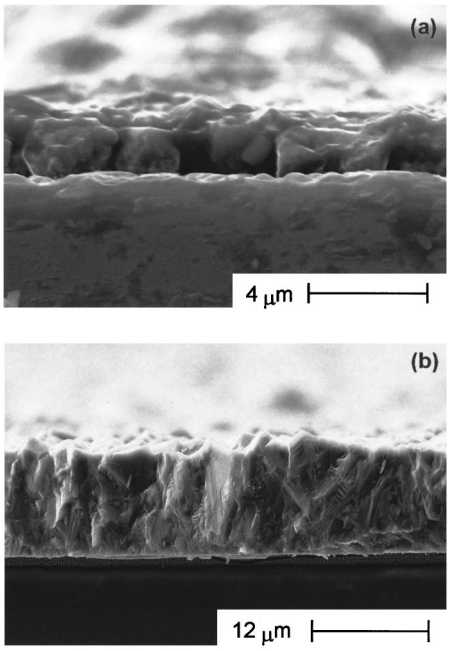

FIG. 2. Cross section scanning electron micrographs of two diamond films with (a) 3.0 and (b) 21 μm, corresponding to Figs. 1(a) and 1(c), respectively. The films are at different growth stages: film (a) is still not completely coalesced exhibiting voids and in film (b) the voids are filled and the columnar growth is evidenced.

of the circle diameter distribution in a representative sample area of around 600 μm^2.

The film thickness was obtained from the cross section micrographs, and was found to vary from 3.0 to 42 μm as the growth time increases from 1.0 to 10 h. Figures 2(a) and 2(b) show, as an example, the cross section of the samples grown during 1.0 and 6.5 h, respectively. The growth evolution can be analyzed from these images. In Fig. 2(a), we do not observe the definitive columnar growth, yet the film is basically formed and needs just to grow in thickness and laterally to fill the voids left behind. The film presents already faceted polycrystalline grains of approximately 1–2 μm in size. As the growth proceeds, the voids are filled and the coalescence of the film is completed until a stage of columnar growth is established. The columnar growth is clearly seen in Fig. 2(b), after 6.5 h of growth. This type of columnar growth, normally considered as a steady state, persists. Morell and co-workers[17] studied recently the evolution of the film microstructure by *in situ* ellipsometry. They have observed a behavior similar to the one described here. Figure 3 shows the average grain size as a function of film thickness, where a linear dependence is clearly observed.

B. X-ray diffraction—sin^2 ψ method

X-ray diffraction is an important, attractive and nondestructive measurement technique that allows evaluating an average stress in a larger sample area when compared to micro-Raman spectroscopy. In addition, the high penetration depth ($\sim$600 μm) of the x-ray beam in diamond allows probing the film throughout its whole depth. The x-ray diffraction measurements were performed in the Philips X'pert-

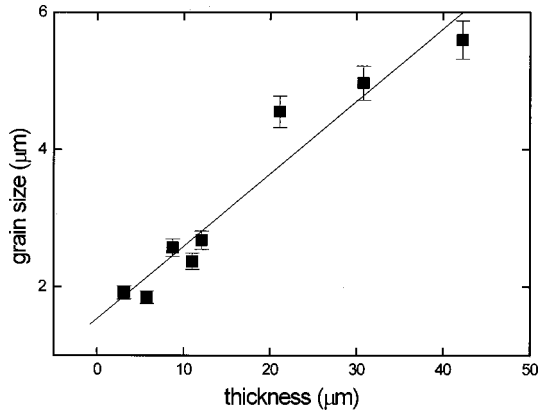

FIG. 3. Grain size, obtained from the analysis of the top view micrographs, as a function of film thickness. A linear behavior is observed.

MRD diffractometer with the Cu x-ray tube in the point focus, a crossed slit collimator (5.0 mm in the horizontal slit, and 1 mm in the axial one) for the incident beam, and a 1 mm receiving slit before the detector.

In order to obtain the total residual stress σ_{total} of the CVD deposited diamond as a function of the film thickness, the sin^2 ψ method[18] was used. This technique consists in measuring the lattice spacing d of a specific (hkl) plane at different tilt angles ψ (inclined exposure). Using these values, the residual stress can be obtained through the relation:

$$\frac{d_\psi - d_0}{d_0} = \frac{1+\nu}{E}\sigma_{total}\sin^2\psi, \tag{1}$$

where E and ν are the Young's modulus and Poisson's ratio of the film, respectively, d_ψ is the lattice spacing at each ψ and d_0 is the d value for $\psi = 0°$ (perpendicular exposure).

In this work, we choose the (331) lattice plane to determine the residual stress in the diamond films. The lattice planes with higher Miller indices (hkl) are normally more sensitive to the residual stress in the film, due to both the steep incidence of x-ray beam (high 2Θ angles) and the small d-values (higher relative variation). Besides that, the shape and intensity of the x-ray curves are expected not to have a significant change with the increase of the tilt angle ψ.

The $\Theta/2\Theta$ scans were measured around the (331) Bragg diffraction peak ($2\Theta \sim 140.6°$) at tilt angles ψ between -60 and $+60°$ for all samples. As an example, Fig. 4 shows the (331) scans for diamond film grown during 6.5 h at three ψ values ($0°$, $+60°$, and $-60°$). Note that each spectrum has two peaks, which are the contribution from the $K\alpha_1$ and $K\alpha_2$ lines. By fitting the (331) x-ray curves with a double Gaussian, the central peak position belonging to the $K\alpha_1$ line were obtained for all ψ values. The lattice spacing d_ψ was then calculated and plotted as a function of the sin^2 ψ, as shown in Fig. 5 for the same sample specified above, evidencing the negative and positive ψ values. The linear behavior observed indicates a homogeneous stress in the film. This fact, together with the small difference in d values obtained for the positive and corresponding negative ψ, reinforces the applicability of the sin^2 ψ method to these diamond films. From the slope of the curve in Fig. 5, the total residual stress is obtained using Eq. (1) with the CVD diamond values of

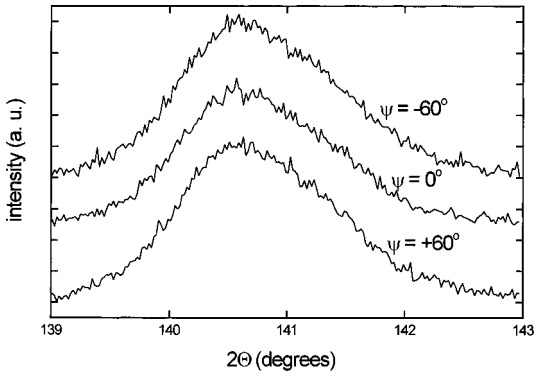

FIG. 4. $\Theta/2\Theta$ scans of the (331) diamond Bragg peak at three different ψ values for a 21 μm thick diamond film. A Gaussian fit was used to deconvolute the Cu$K\alpha_1$ peak.

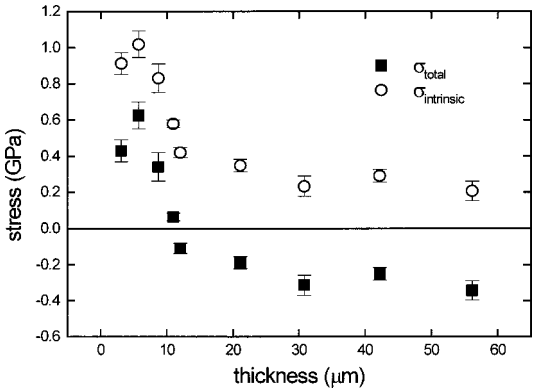

FIG. 6. Total residual stress σ_{total} and the intrinsic component $\sigma_{\text{intrinsic}}$ as a function of film thickness for our diamond films.

1250 GPa for E and 0.07 for ν[9]. The negative slope in this plot indicated that the residual stress in the film is compressive.

During the cooling from growth temperature (T_g) to room temperature (T_{amb}), a thermal stress is built-up due to the difference in the thermal expansion coefficient α between the diamond film and the Si substrate. In order to obtain the intrinsic stress, the thermal stress has to be subtracted from the total stress. The thermal stress can be calculated using the following relation:[19]

$$\sigma_{\text{thermal}} = \int_{Tg}^{T_{\text{amb}}} E/(1-\nu)[\alpha_{\text{diamond}}(T) - \alpha_{\text{Si}}(T)]dT, \quad (2)$$

where α(T) is the temperature dependence of the thermal expansion coefficient of silicon and diamond,[20] E and ν have the same meaning as in equation (1). Using the value of the biaxial Young's modulus, $E/(1-\nu)$, of 1345 GPa,[9] a constant and compressive thermal stress $\sigma_{\text{th}} = -0.52$ GPa was found for the deposition temperature used (1070 K).

The total residual stress σ_{total}, obtained from the $\sin^2\psi$ method for all samples, is plotted in Fig. 6 as a function of film thickness, together with the intrinsic stress component $\sigma_{\text{intrinsic}}$ (open circles). Note that the total residual stress starts tensile at a value of ~ 0.6 GPa, changes from tensile to compressive for films thicker than around 10 μm, and remains compressive at approximately -0.3 GPa up to a film thickness of 42 μm. Observe that the intrinsic stress, obtained from these data, is always tensile. The error bars in this graph were evaluated from the standard deviation to the linear regression in the $\sin^2\Psi$ plot (Fig. 5).

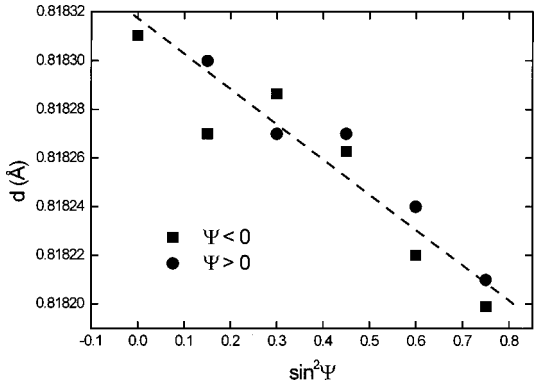

FIG. 5. Lattice spacing d versus $\sin^2\psi$ for the 21 μm diamond film. The negative slope indicated a compressive residual stress.

C. Raman spectroscopy

The shift of stressed diamond Raman line relative to the natural diamond line at 1332 cm^{-1} has been used by many authors in order to calculate the total residual stress in diamond films.[20–22] In addition to the stress evaluation, the analysis of the Raman spectra gives lot information about the film properties, especially concerning the film purity.

Using a Renishaw microscopic system 2000, micro-Raman spectra were recorded in backscattering configuration at room temperature employing the argon–ion laser excitation line (514.5 nm). The laser beam was focused on the sample using two objectives with different magnifications (20× and 50×), leading to two different spot sizes. The 20× magnification corresponds to a spot of ~ 2.0 μm in diameter, and the 50× to a spot of ~ 5.0 μm. The penetration depth is estimated to be approximately 5.0 μm in both cases.

The goal of this procedure is to compare the average results when a larger probe area is analyzed in the same experimental conditions. Besides, a single micro-Raman measurement point is not representative for the stress evaluation in diamond films due to the presence of highly inhomogeneous stresses. Therefore, a large number of spectra were recorded from a selected area and added (summation method). Five points in the sample were chosen in a central area of 4.0 mm^2. For each point in such area, the spectra were scanned five times, in order to improve the statistics of Raman data.

Figure 7 shows the micro-Raman spectra, obtained from the focalized spot of 2.0 μm, of two diamond films with thickness of 3.0 and 21 μm (spectrum 1 and 2), that correspond to the samples of Figs. 2(a) and 2(b), respectively. The Raman spectra of all samples exhibited, in addition to the evident diamond peak at 1332 cm^{-1}, a broadband centered at around 1560 cm^{-1}, which is attributed to disordered graphitic carbons. The increasing background, clearly observed in all Raman spectra, is due to the photoluminescence of the

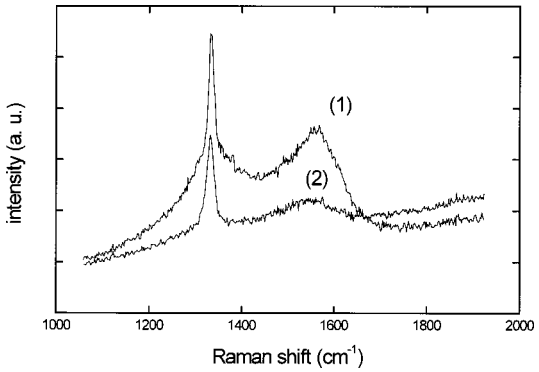

FIG. 7. Micro-Raman spectra of two diamond films with thickness of 3.0 μm (curve 1) and 21 μm (curve 2). Both spectra exhibit the diamond line at 1332 cm^{-1} and a broad band centered at around 1550 cm^{-1} relative to the graphitic phases.

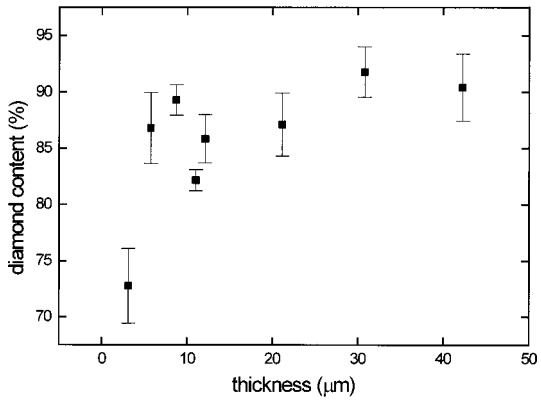

FIG. 8. Amount of diamond relative to graphite (diamond purity), obtained from the quantitative analysis of the Raman spectra, as function of film thickness.

graphite phase. Note, also, that the intensity of the graphite band relative to the diamond line increases for decreasing film thickness. This fact can be explained by the relative higher concentration of nondiamond phase material, which is normally accumulated in spaces between the crystalline grains during the initial process of growth. The Raman spectra measured with the spot size of 5.0 μm showed similar results, presenting differences only in the line intensities.

The relative amount of diamond in the film, also called diamond purity, can be obtained by a quantitative analysis of the Raman spectrum. To separate the contributions of diamond and disordered graphitic phases to the total Raman scattering, the whole Raman spectrum were fitted with Lorentzian lines, using the luminescence contribution as an exponential grown base line. To fit the broad band centered at 1550 cm^{-1}, it was necessary to take three different contribution bands: the D and G peak of polycrystalline graphite at around 1345 and 1560 cm^{-1}, and a low intensity band centered approximately at 1470 cm^{-1} attributed to a tetrahedrally bonded diamond precursor. The amount of diamond in the films can be calculated by a relative Raman cross section of diamond to graphite of 1/50 by the relation:[21]

$$C_d = 100\, A_d \Big/ \left(A_d + \frac{\Sigma A_i}{50} \right), \tag{3}$$

where A_d and A_i are the area of the fitted curves corresponding to the 1332 cm^{-1} diamond peak and the graphitic bands, respectively. This procedure was accomplished for all grown films, and Fig. 8 shows the result as function of film thickness. The relative amount of diamond increases approximately from 73% to 92% as the film thickness goes from 3 to 10 μm, remaining at the value of $\sim$90% up to 40 μm. This behavior is expected since, as discussed above, the concentration of graphitic materials at the grain boundaries is higher for the thinner films, and the micro-Raman spectroscopy probes only the first 5 μm from the film surface.

Let us now determine the residual stress from the diamond Raman line shifts. There is a controversy in the literature about the dependence of the diamond Raman line shift on applied pressure. Measurements on both natural diamond[23] and SHOCK DIAM,[24] which consist of diamond crystallites with different grain sizes, lead to a linear shift of 2.9 cm^{-1}/GPa. Values even three times smaller[25] can be found in the literature. We use the value of SHOCK DIAM [27] because of its similarity in the form to the CVD grown diamond films. This value leads to the relation:

$$\sigma \cong -0.345 \text{ GPa/cm}^{-1}, \tag{4}$$

where $\Delta\nu$ is the shift of the Raman peak of diamond films with respect to that of natural diamond. A positive (or negative) $\Delta\nu$ corresponds to a compressive (or tensile) stress.

Figure 9 shows, as an example, four expanded Raman spectra around the diamond peak of three samples with thickness of 3.0 (curve 1), 12 (curve 2) and 42 μm (curve 3) together with a reference spectrum of natural diamond (curve 4). The peak shift is clearly evidenced in this graph, showing a tensile stress for the 3 μm film and a compressive residual stress for the other two spectra. The residual stress was calculated, following this procedure, for all measured Raman spectra of each sample. Figure 10 presents this result as a function of film thickness for the two spot sizes: 2.0 μm (solid square) and 5.0 μm (open circle). The error bar is the mean square deviation obtained from the five measurements in different places of the sample. From this graph, one can observe that the residual stress starts compressive (around -0.7 GPa) for a 3 μm thick film, decreases to approximately

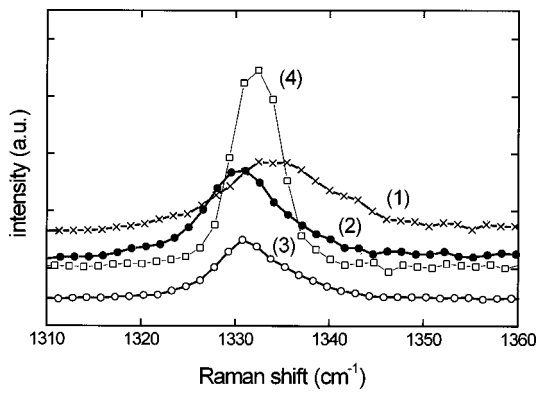

FIG. 9. Expanded Raman spectra around the diamond peak for three samples with thickness of 3.0 (curve 1), 12 (curve 2), 42 μm (curve 3), and for a reference natural diamond (curve 4). The peak shift is evidenced in this plot.

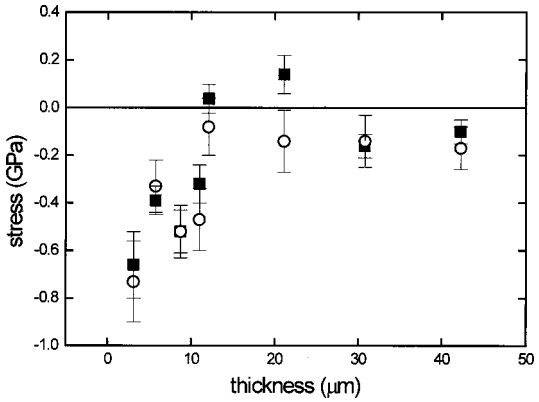

FIG. 10. Total residual stress in the diamond films as a function of thickness evaluated from the Raman peak shift in the spectra measured with the spot size of 2.0 (solid squares) and 5.0 μm (open circles). No appreciable difference is found in the results obtained from the two spot sizes.

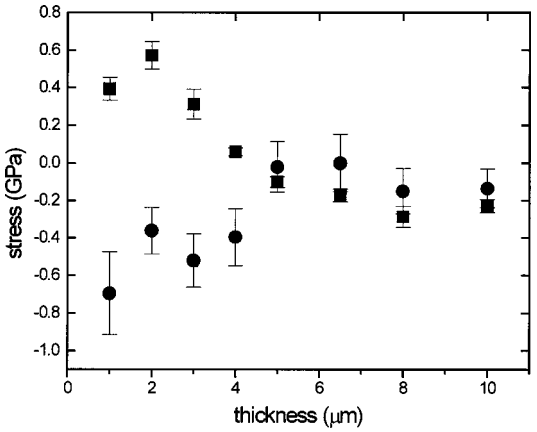

FIG. 12. Comparison between the total residual stress obtained from x-ray diffraction (solid square) and Raman spectroscopy (open circle). The Raman data is the average result obtained with the two spot sizes (2.0 and 5.0 μm). A good agreement is found for films thicker than 10 μm, while an opposite behavior is observed for the thinner samples.

zero (or even to a small value of tensile stress). When the film thickness reaches 12 μm, returns to a compressive value at around -0.2 GPa, and stays at this value up to 42 μm. No appreciable difference was found for the measurements made with the two spot sizes. Comparing with the results obtained from the x-ray data, an opposite behavior is found for films thinner than 10 μm, but a good agreement between x-ray and micro-Raman analysis is observed for films in the range from 10 to 40 μm.

As can be seen in Fig. 9, the width of the Raman diamond line increased with decreasing film thickness. We tried to correlate the stress, obtained from the line shift, with the full width at half maximum (FWHM) of the Raman line. Figure 11 plots this result, and a linear dependence is found in the compressive stress region.

IV. DISCUSSION AND CONCLUSION

The comparison between the residual stress obtained from the x-ray measurements and micro-Raman analysis is plotted in Fig. 12. For the Raman data, an average between the results obtained with the 2.0 and 5.0 μm spot sizes is displayed. As discussed above, accordance is found for films in the range of 10 to 40 μm, and for thinner samples both results diverge.

Our stress data shown in Fig. 12 follow the trend found in the literature.[26–28] A compressive stress is dominant in the early stage of film growth, mainly due to the thermal stress. As the film becomes thicker, the stress changes to tensile, and for thicker films the stress tends to saturate in a small compressive or tensile value, depending on the film characteristics. Since our films were always thicker than 3.0 μm, we did not investigate the stage before the coalescence of the film.

We cannot establish here the fundamental reasons of the discrepancy found between the results obtained with the x-ray and Raman measurements for films thinner than 10 μm, but we believe it is associated to the domain size characteristic of each measurement technique. In the x-ray technique, the x-ray beam is scattered by the crystalline part of the diamond grain, and the effect of lattice distortion is averaged over a large sample area through the whole depth of the film. In contrary, the micro-Raman spectroscopy is a local technique that probes only the spot-size area with a penetration of 5.0 μm from the surface. In the region where the grain size is smaller than the Raman spot size, the relative contribution of the grain boundaries (which is compressive) to the stress measurement is higher. As the grain size increases with film thickness, both results tend to converge, since the boundaries become less and less important.

Independent of this result, micro-Raman spectroscopy is a powerful and sensible technique. In spite of its contribution arises from small sample area and penetration depth, micro-Raman measurement permits an analysis of impurities and defects, especially the ones associated to graphitic phases. This sensitivity is very useful to obtain other important parameters of the diamond film. Our results also show that care must be taken when measuring micro-Raman to calculate residual stress. It is necessary to make a good statistics in different points of sample in order to obtain reliable values. Another source of error in the stress evaluation is the varia-

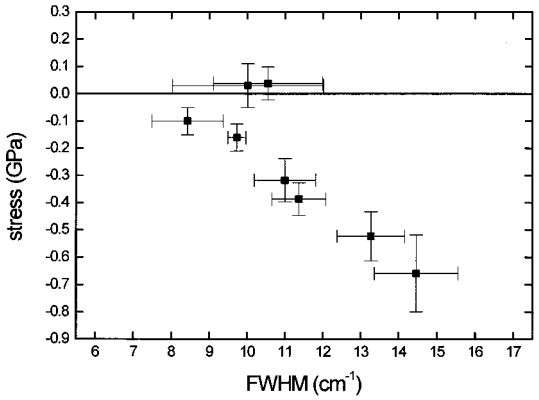

FIG. 11. Correlation between the full width at half maximum (FWHM) and the stress value obtained from the diamond Raman line for the spot size of 2.0 μm.

tion of the diamond Young's modulus with film quality, which is normally not considered.

In conclusion, the determination of residual stress in diamond films still remains a controversial subject, with results depending strongly on the measurement technique. This work establishes at least some domain regions where the results are more probable to converge.

[1] V. J. Trava-Airoldi, E. J. Corat, E. Del Bosco, and N. F. Leite, Surf. Coat. Technol. **76–77**, 797 (1995).
[2] V. J. Trava-Airoldi, E. J. Corat, and V. Baranauskas, in *Advanced Ceramics Tools for Machining Application III*, edited by I. M. Low (Trans Tech Publications, Uetikon-Zuerich, Switzerland), Vol. 138–140, Chap. 6, p.195.
[3] N. G. Ferreira, E. Abramof, E. J. Corat, N. F. Leite, and V. J. Trava-Airoldi, Diamond Relat. Mater. **10**, 750 (2001).
[4] N. G. Ferreira, L. L. G. Silva, E. J. Corat, and V. J. Trava-Airoldi, Diamond Relat. Mater. (submitted).
[5] V. J. Trava-Airoldi, A. F. Azevedo, E. J. Corat, J. R. Moro, N. F. Leite, published in the Book Series, *Frontiers in Interdisciplinary Physics* (IAPS Press, La Jolla, CA, 1998).
[6] H. Windischmann and G. F. Epps, J. Appl. Phys. **69**, 2231 (1991).
[7] D. Rats, L. Bimbault, L. Vandenbulcke, R. Herbin, and K. F. Badawi, J. Appl. Phys. **78**, 4994 (1995).
[8] M. Hempel and M. Harting, Diamond Relat. Mater. **8**, 1555 (1999).
[9] H. Windishchmann and K. J. Grey, Diamond Relat. Mater. **4**, 837 (1995).
[10] R. J. Nemanich, L. Bergman, Y. M. LeGrice, K. F. Turner, and T. P. Humphreys, Proc. SPIE **1437**, 2 (1991).
[11] Y. H. Lee, K. J. Bachmann, J. T. Glass, Y. M. LeGrice, and R. J. Nemanich, Appl. Phys. Lett. **57**, 1916 (1990).
[12] M. Yoshikawa, G. Katagri, H. Ishida, A. Ishitani, M. Ono, and K. Matsumura, Appl. Phys. Lett. **55**, 2608 (1989).
[13] H. Guo and M. Alam, Thin Solid Films **212**, 173 (1992).
[14] S. A. Stuart, S. Prawer, and P. S. Weiser, Appl. Phys. Lett. **62**, 1227 (1993).
[15] P. K. Bachmann, H. Lade, D. Leers, and D. U. Wiechert, Diamond Relat. Mater. **3**, 799 (1994).
[16] R. C. Mendes de Barros, E. J. Corat, N. G. Ferreira, T. M. Souza, V. J. Trava-Airoldi, N. F. Leite, and K. Iha, Diamond Relat. Mater. **5**, 1323 (1996).
[17] G. Morell, L. M. Cancel, O. L. Figueroa, J. A. Gonzales, and B. R. Weiner, J. Appl. Phys. **88**, 5716 (2000).
[18] I. C. Noyan, T. C. Huang, and B. R. York, Crit. Rev. Solid State Mater. Sci. **20**, 125 (1995).
[19] G. A. Slack and S. F. Bartram, J. Appl. Phys. **46**, 89 (1975).
[20] Y. von Kaenel, J. Stiegler, J. Mitchler, and E. Blank, J. Appl. Phys. **81**, 1726 (1997).
[21] W. L. Wang, M. C. Polo, G. Sanchez, J. Cifre, and J. Esteve, J. Appl. Phys. **80**, 1846 (1996).
[22] J. G. Kim and J. Yu, Scr. Mater. **39**, 807 (1998).
[23] H. Boppart, J. van Straaten, and I. F. Silvera, Phys. Rev. B **32**, 1423 (1985).
[24] M. J. Lipp, V. G. Baonza, W. J. Evans, and H. E. Lorenzana, Phys. Rev. B **56**, 5978 (1997).
[25] M. Schreck, H. Roll, J. Michler, E. Blank, and B. Stritzker, J. Appl. Phys. **88**, 2456 (2000).
[26] M. Janda and O. Stefan, Thin Solid Films **112**, 127 (1984).
[27] R. P. Vinci and J. C. Bravman, Mater. Res. Soc. Symp. Proc. **428**, 481 (1996).
[28] F. A. Doljak and R. W. Hoffmann, Thin Solid Films **12**, 71 (1972).